

Iowa State University

From the Selected Works of Vinay Dayal

January, 1989

Dynamic Young's Modulus Measurements in Metallic Materials: Results of an Interlaboratory Testing Program

A. Wolfenden, *Texas A&M University, College Station*

M. R. Harmouche, *Texas A&M University, College Station*

G. V. Blessing, *National Bureau of Standards*

Y. T. Chen, *Pitney Bowes*

P. Terranova, *Pitney Bowes*, et al.



Available at: https://works.bepress.com/vinay_dayal/26/

A. Wolfenden,¹ M. R. Harmouche,¹ G. V. Blessing,² Y. T. Chen,³ P. Terranova,³ V. Dayal,⁴ V. K. Kinra,⁵ J. W. Lemmens,⁶ R. R. Phillips,⁷ J. S. Smith,⁸ P. Mahmoodi,⁹ and R. J. Wann⁹

Dynamic Young's Modulus Measurements in Metallic Materials: Results of an Interlaboratory Testing Program

REFERENCE: Wolfenden, A., Harmouche, M. R., Blessing, G. V., Chen, Y. T., Terranova, P., Dayal, V., Kinra, V. K., Lemmens, J. W., Phillips, R. R., Smith, J. S., Mahmoodi, P., and Wann, R. J., "Dynamic Young's Modulus Measurements in Metallic Materials: Results of an Interlaboratory Testing Program," *Journal of Testing and Evaluation*, JTEVA, Vol. 17, No. 1, Jan. 1989, pp. 2-13.

ABSTRACT: The results of a round-robin testing study are presented for measurements of dynamic Young's modulus in two nickel-based alloys. The Interlaboratory Testing Program involved six types of apparatus, six different organizations, and specimens from a well-documented source. All the techniques yielded values of dynamic Young's modulus that agreed within 1.6% of each other. For Inconel alloy 600 the dynamic modulus was 213.5 GPa with a standard deviation of 3.6 GPa; for Incoloy alloy 907 the corresponding values were 158.6 and 2.2 GPa, respectively. No significant effect of frequency over the range 780 Hz to 15 MHz was found.

KEY WORDS: elastic modulus, dynamic, Young's modulus, metals, interlaboratory, frequency dependence

In engineering and science elastic modulus is of fundamental and technological importance. It has applications in areas such as load-deflection, buckling, thermoelastic stresses, elastic instability, fracture mechanics, creep, interatomic potentials, lattice defects, thermodynamic equations of state, free energy, and thermal expansion.

In reflection of this wide-ranging importance of modulus, several standards organizations around the world have formulated procedures for the determination of static and dynamic modulus of

certain types of materials. For example, ASTM has published Standard Methods for Young's Modulus, Shear Modulus, and Poisson's Ratio for Glass and Glass-Ceramics by Resonance (ASTM C 623), Young's Modulus, Shear Modulus, and Poisson's Ratio for Ceramic Whitewares by Resonance (ASTM C 848), Moduli of Elasticity and Fundamental Frequencies of Carbon and Graphite Materials by Sonic Resonance (ASTM C 747), and Fundamental Transverse, Longitudinal, and Torsional Frequencies of Concrete Specimens (ASTM C 215). In addition, there is the well-known standard test method for determining static Young's modulus of metallic tensile specimens (ASTM E 111). In view of the considerable amount of work devoted by members of standards organizations to the formulation and publication of these recognized testing methods for specific materials, it is very surprising that *there is no recognized testing method for the determination of dynamic Young's modulus in metallic materials*. There is, however, a large contribution towards a recognized testing method for dynamic modulus in ASTM Practice for Measuring Ultrasonic Velocity in Materials (E 494). The main aim of this paper is to be a part of a movement to fill this lacuna.

As background history to the preparation of this paper, it is pertinent to mention that in the early 1980s, within the framework of ASTM Subcommittee E28.03 on Elastic Properties and Definitions on Mechanical Testing, an Interlaboratory Testing Program was set up to address measurements of dynamic Young's modulus in metals. This program or task group carries the identification E28.03.05; its active members and their laboratories are listed in Table 1. The paper is the first full report resulting from the testing program and documents the alloys used as specimens, some details on the various testing techniques in the laboratories, the experimental results, a detailed analysis of the results (with discussion), and the conclusions of the study.

Specimens

For the Interlaboratory Testing Program special care was devoted to specimen selection and preparation. An early discussion of the ASTM E28.03.05 group resulted in a consensus that the materials chosen should be of technological interest and that the preference of one of the laboratories for a magnetic material should be respected. One of the group members made the resources of his company available in this regard. Thus Inco Alloys International provided both the materials and the machining facilities. The metallic materials chosen for the tests were Inconel alloy 600 (UNS N06600; designated Alloy A) and Incoloy alloy 907 (UNS N19907;

Manuscript received 3/15/87; accepted for publication 7/15/88.

¹Mechanical Engineering Department, Texas A&M University, College Station, TX 77843.

²Ultrasonics Standards Group, National Bureau of Standards, Gaithersburg, MD 20899. (The National Bureau of Standards is now the National Institute of Standards and Technology.)

³Corporate R&D, % Zell #1, Pitney Bowes, Walter H. Wheeler, Jr. Dr., Stamford, CT 06904.

⁴Department of Mechanical Engineering, North Carolina A&T State University, Greensboro, NC 27411.

⁵Aerospace Engineering Department, Texas A&M University, College Station, TX 77843.

⁶Elektronika N.V., Research Park 62, B-3030 Leuven, Belgium.

⁷348 Center Street, St. Marys, PA 15857.

⁸Inco Alloys International, Inc., P.O. Box 1958, Huntington, WV 25720.

⁹Corporate Research Laboratories/3M, 3M Center, St. Paul, MN 55133.

0090-3973/89/0001-0002\$00.00

TABLE 1—List of the personnel taking part in the interlaboratory testing program and their laboratories or company names, and of the trade names or acronyms (where available) for the apparatus used and the physical principle of operation.

Laboratory	Personnel	Trade Name or Acronym	Physical Principle
1. Inco Alloys International	J. S. Smith		Free-free Beam (F)
2. Pitney Bowes	Y. T. Chen R. R. Phillips P. Terranova		Free-free Beam (F)
3. J. W. Lemmens Elektronika	J. W. Lemmens	Grindo-Sonic	Impulse Excitation (F)
4. National Bureau of Standards (NBS)	G. V. Blessing		Velocity Measurements of Ultrasonic Wave Pulses (T)
5. Texas A&M University	A. Wolfenden M. R. Harmouche	PUCOT (Piezoelectric Ultrasonic Composite Oscillator Technique)	Piezoelectric Ultrasonic Oscillation (F)
6. Texas A&M University	V. K. Kinra V. Dayal		Ultrasonic Pulse Spectroscopy (P)
7. 3M Company	P. Mahmoodi R. J. Wann		Free-free Beam (F)
8. Texas A&M University	A. Wolfenden M. R. Harmouche	Modul-R	Magnetically Excited Resonance (F)

F: Denotes that the apparatus is designed to measure frequency of the specimen.

T: Denotes that the apparatus is designed to measure the transit time for ultrasonic pulses.

P: Denotes that the apparatus is designed for ultrasonic pulse spectroscopy.

the magnetic material, designated Alloy B).¹⁰ The chemical compositions, thermomechanical treatments, and sizes of the specimens of Alloys A and B are given in Table 2. The specimen sizes reflect to a great extent the optimum or convenient sizes pertinent to the particular measuring techniques at the various laboratories. To examine the possibility that the specimens were *not* isotropic, X-ray diffraction pole figures (powder patterns) were obtained for filings from the specimens and for pieces of the specimens. For Inconel alloy 600 (Alloy A), no significant texture effects were detected. However, for Incoloy alloy 907 (Alloy B), small traces of (311) and (222) textures were found.

Experimental Procedures

All experimental methods of measuring dynamic Young's modulus E use, in some form or other, the basic wave equation for the propagation of a longitudinal elastic wave in an elastic medium:

$$E = \rho v^2 \quad (1)$$

where ρ is the mass density of the medium and v is the wave speed.

¹⁰Inconel and Incoloy are trademarks for products of the Inco family of companies (Inco Alloys International, Inc.).

Thus the methods that are concerned with measurements of transit time t (and hence velocity) of ultrasonic pulses over a known distance L in an elastic medium apply Eq 1 directly ($v = L/t$), assuming that ρ is known or can be measured also. In the case of the methods that utilize measurements of resonant frequency of standing or decaying elastic waves in an elastic medium a modified form of Eq 1 is applied:

$$E = \rho v^2 = \rho (f\lambda)^2 \quad (2)$$

where f is the resonant frequency and λ is the wavelength. The specific geometrical details of the specimen usually determine λ . For example, for a uniform beam resonating in its fundamental longitudinal mode, the wavelength is twice the length L of the beam. Therefore Eq 2 becomes

$$E = 4\rho L^2 f^2 \quad (3)$$

Again, in the frequency methods ρ must be known or measured. All but one of the experimental procedures used in the Interlabora-

TABLE 2—Chemical compositions, thermomechanical treatments, and sizes of the specimens of Alloys A and B.

	Alloy A (Inconel Alloy 600)	Alloy B (Incoloy Alloy 907)
Composition (wt%)		
Ni	74.91	37.46
Cr	15.48	...
Fe & others	balance	balance
C	0.08	0.01
Co	...	14.38
Nb	...	4.71
Ti	...	1.46
Treatment		
	Cold drawn	Hot rolled
	Mill annealed ^a	
	31.75 mm	17.78 by 101.6 mm
	(1.25 in.) diameter	(0.7 by 4 in.) flat
Specimen Sizes		
Round	6.35 mm (0.25 in.) diameter by 79.38 mm (3.125 in.) long	
Strip	2.03 mm (0.080 in.) by 6.35 mm (0.25 in.) by 106.65 mm (4.199 in.)	
Special #1	25.4 mm (1.000 in.) diameter by 101.6 mm (4.000 in.)	
Special #2	50.8 by 50.8 by 19.05 mm (2 by 2 by 0.750 in.) 25.4 mm diameter by 19.05 mm (1 in. diameter by 0.750 in.)	

^aIn the range 980 to 1038°C.

tory Testing Program fell into these two basic categories for determining dynamic Young's modulus. The third basic technique, newly developed, is ultrasonic pulse spectroscopy. The techniques will be described in this section of the paper in the following sequence: free-free beam, impulse excitation, wave velocity measurements, ultrasonic pulse spectroscopy, piezoelectric ultrasonic oscillation, and magnetically excited resonance.

Free-Free Beam Technique

Three of the laboratories mentioned in Table 1 incorporated the free-free beam test method [1-3]. While the details of the apparatus at the three locations vary, the basic principle of operation is the same. For brevity, an apparatus will be described which may be regarded as typical for the technique.

The test method is patterned after the technique of Spinner and Tefft [2] of the National Bureau of Standards. Figure 1 shows schematically the instrumentation and the test configuration. The rectangular or cylindrical specimen is suspended near its nodal points by pure silk or cotton-covered polyester thread. The nodal points for beams of uniform section in a free-free suspension are at distances from the free ends of approximately $0.22L$ and $0.78L$ [4]. For the rectangular specimen the cotton threads are positioned at opposite sides as indicated by Spinner and Tefft [2] and suspended from Astatic X 26 crystal cutters used as both drive and pickup transducers. This configuration of opposite side suspension excites both the flexural and torsional modes of vibration. Cylindrical specimens are suspended in a similar manner except for the obvious off-setting of the suspension positions. Alternatively, the better

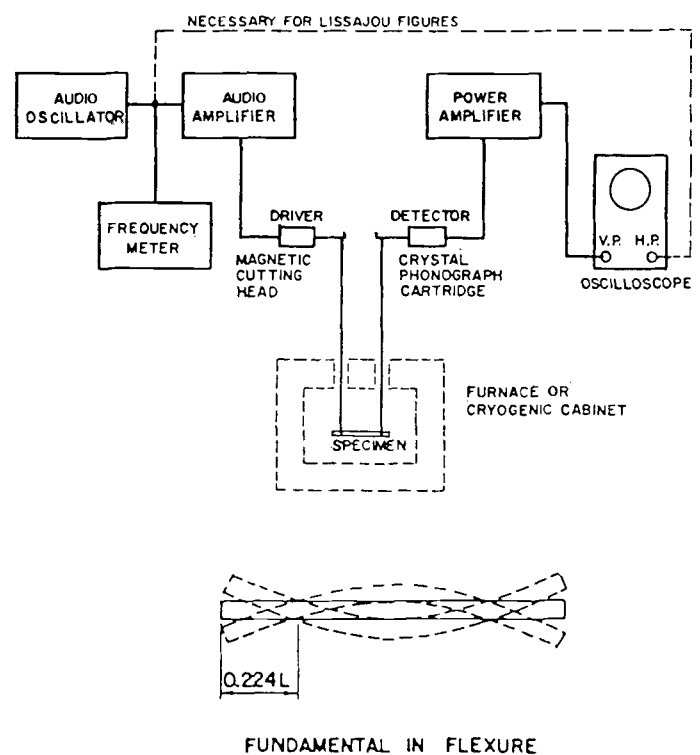


FIG. 1—Schematic diagram of the instrumentation used in the free-free beam test method and of the test configuration. The specimen is suspended at or near the nodal points.

string suspension system known as the loop method may be used [5].

The sine wave signal from a function generator is fed to a power amplifier and then to the driver transducer. The pickup transducer has a $10\times$ gain preamplifier. The signal from the pickup is analyzed on a suitable analyzer, which is configured in a peak averaging mode using exponential averaging. The function generator is swept manually through the frequency range of interest while the output signal is examined. The fundamental frequency is quite easily determined in this manner.

Physical measurements such as length, width, diameter, or thickness are measured with a machinist's caliper. The density of the specimen is determined using mass and volume calculated from the measured dimensions.

The equations used for calculating Young's modulus are [4]

$$\text{Cylindrical: } E = 64\pi^2 f^2 L^4 \rho / A^2 d^2 \quad (4)$$

$$\text{Rectangular: } E = 48\pi^2 f^2 L^4 \rho / A^2 h^2 \quad (5)$$

where

f = fundamental frequency,
 L = free length,
 ρ = density,
 d = diameter,
 h = thickness, and
 A = constant depending on the shape of the specimen.

Impulse Excitation Technique

The test method entails (a) the excitation of the test specimen by means of a light mechanical impulse (a tap) and (b) the analysis of the resultant transient vibration. An electronic circuit is used to

isolate the harmonics and the fundamental resonant frequency from the spectrum of noise, and to measure the period corresponding to the fundamental frequency. The result is displayed in digital form. A block diagram for the method is shown in Fig. 2.

The specimen is supported preferably at the nodes of the desired vibrational mode. By positioning correctly the location of the exciting impulse, each mode can be induced easily. Whatever the mode, the instrument will identify the fundamental resonant frequency of the vibration. Very little exciting energy is required, even for very large specimens, because the measurement is performed at a very low strain amplitude. Hence only a very light tap is sufficient to initiate the measurement.

The most versatile means of detecting the vibrational motion is provided by a hand-held piezoelectric probe. It is used to analyze signals from about 20 Hz to 80 kHz in frequency. Acoustic, optical, or electromagnetic detectors can be used for specialized purposes, such as testing materials at high temperatures. With the fundamental resonant frequency thus obtained and the density determined by the Archimedes method, the moduli and Poisson's ratio can be calculated for regular shaped specimens using well-known equations [2].

Velocity of Ultrasonic Wave Pulses

This technique is one of the better known methods for measuring dynamic moduli in materials. A brief account of the theory behind the technique and of the experimental arrangement is given.

For ultrasonic wavelengths less than the dimensions of the specimens, two normal modes of wave propagation in isotropic media prevail. They are the longitudinal and shear modes, with respective velocities V_L and V_S (see, for example, Refs 6 and 7 and ASTM E 494). Longitudinal waves, sometimes referred to as compressional waves, alternately compress and dilate the material lattice (i.e., generate compressive and tensile strains) as they pass by. The re-

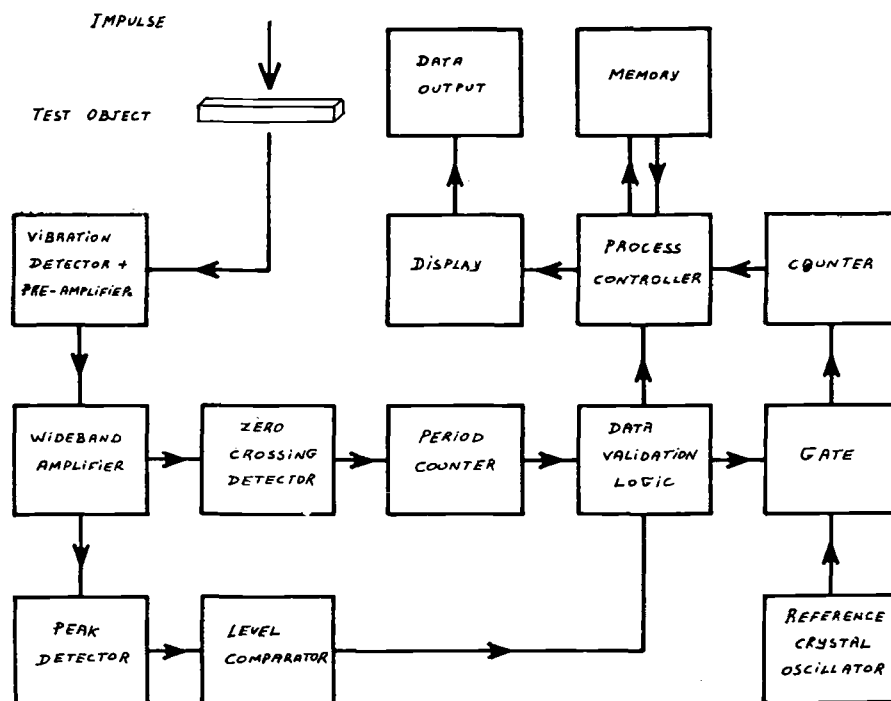


FIG. 2—Block diagram of the impulse excitation technique.

sulting particle motion of the material is parallel to the direction of wave propagation. Shear waves, on the other hand, generate particle displacements perpendicular to the propagation direction, causing the material lattice to shear as the waves pass by.

From these two wave speeds and the density ρ , all the elastic parameters of the material can be calculated: the Young's, bulk, and shear moduli, and Poisson's ratio (P.R.). Their relationships are given by

$$\text{Young's modulus} = \rho V_s^2 (3V_L^2 - 4V_s^2) / (V_L^2 - V_s^2) \quad (6)$$

$$\text{Bulk modulus} = \rho (V_L^2 - (4/3) V_s^2) \quad (7)$$

$$\text{Shear modulus} = \rho V_s^2 \quad (8)$$

$$\text{P.R.} = (V_L^2 - 2V_s^2) / (2V_L^2 - 2V_s^2) \quad (9)$$

Anisotropy and inhomogeneity in the specimen may be conveniently evaluated ultrasonically. If a specimen is inhomogeneous, different wave speeds will be observed at different positions in the specimen; if the specimen is anisotropic, different wave speeds will be observed for different propagation directions in the specimen. Furthermore, shear waves may be used to evaluate anisotropy in the specimen by propagating them in the same direction and rotating the transducer's particle displacement (polarization) vector.

The wave speed V in the specimen is determined by measuring the transit time t of an ultrasonic pulse over a known path L in the specimen, and by calculating $V = L/t$. It is important to note that the distinction between phase and group velocities becomes irrelevant for non-dispersive media, such as the specimens tested here. This is pointed out empirically in the following section. The necessary measurements to differentiate between group and phase values were not made. The measurement techniques applied here could span the difference between the two values. In any event, the difference between the values is probably less than the measurement precision quoted for the metal samples studied: one part in a thousand, or 0.1%. Typically, L is twice some usable dimension in the specimen, such as the cylinder bar length or the thickness of a flat strip. The factor of two derives from the round-trip distance for the pulse when making pulse-echo measurements using a single

transducer. The pulse-echo-overlap technique is convenient for making precise transit time measurements [8]. With this technique, at least two echoes (with a single transducer) are needed to provide an overlap of successive echoes on the oscilloscope by means of time-delaying circuitry, from which the transit times in the specimen are determined.

The ultrasonic velocity measurements are made at frequencies ranging from 5 to 15 MHz for the specimen dimensions in these tests, with the higher frequencies being used for shorter path lengths. All measurements are made at a nominal room temperature of 21°C. Figure 3 illustrates the principal components used for a majority of the measurements. (Some data are taken using a through-transmission technique wherein a second transducer attached to the opposite face of the specimen receives the ultrasonic pulse.) A pulser/receiver unit transmits a very short (less than 0.1 μ s) spike voltage to a transducer, generating a broad-band ultrasonic wave of short duration—less than 1.0 μ s, for example, at 5 MHz. A typical broad-band wave shape is illustrated in Fig. 3. For the rod sample, it should be noted that the errors in determining wave speed can be very significant due to sidewall reflections using the pulse-echo-overlap (or through transmission) technique [9]. Alternatively, the transducer may be driven by a multi-cycle sinusoidal voltage burst, usually at the transducer's resonant frequency, which results in a relatively narrow band ultrasonic wave packet of longer duration—several microseconds, for example, at 5 MHz. The transducer converts the excitation into a mechanical oscillation or sound wave which is coupled into the specimen to propagate at the sound velocity. The coupling is significantly enhanced by use of a thin layer (much less than an ultrasonic wavelength) of liquid or elastomer material. (Other coupling techniques exist which do not require direct mechanical contact of transducer to specimen [7].) Commercially available transducers have a casing that houses a piezoelectric element and often an impedance matching circuit, which are designed for convenient electrical attachment to the pulser/receiver via coaxial cable and standard connectors. The piezoelectric elements of the transducers used in this work range from 4 to 13 mm diameter.

After entering the specimen, the ultrasonic pulse echoes back and forth between the faces of the specimen, while constantly decaying in amplitude due to scattering, absorption, and boundary

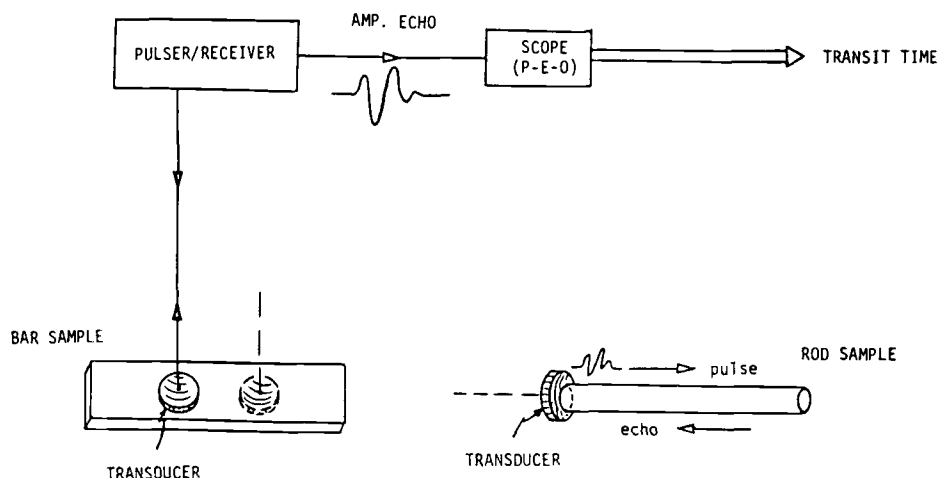


FIG. 3—Ultrasonic velocity measurement system with direct contact of transducer on specimen. The transit time of the ultrasonic pulse is measured by the pulse echo overlap technique.

interface losses. Each time the wave pulse is incident at the transducer/specimen interface, a portion of the elastic wave energy is converted into an electrical signal by the transducer. This received signal is then amplified and displayed on an oscilloscope so that the transit time measurements can be made. Electronic techniques exist to automate the measurements with direct computer control. The accuracy of these measurements depends on the dimensions of the specimen (path length, end-face parallelism, etc.), the particular ultrasonic coupling technique, and the signal-to-noise ratio. Typically, the accuracy for these transit time measurements is $\pm 0.1\%$ or better. The accuracy could be increased (if desired) by taking into account (a) the effects of beam spreading (diffraction) and (b) the small but finite effect of the bond layer thickness on the phase shift upon each reflection from the specimen-transducer boundary, as noted elsewhere [10,11]. However, in discussing these potentially high accuracies, the limitations imposed by the inhomogeneity and anisotropy of the specimens should be kept in mind. Indeed, in Specimen 2.3 (Incoloy alloy 907) a noticeable anisotropy of about 10% for the shear modulus was detected at both Positions 1 and 2 (see Fig. 3, bar sample). This anisotropy effect on the modulus most likely arises from the texture observed in Alloy B (see Specimens section). The densities of the specimens for this study were determined by the Archimedes method, by which the density of the specimen is measured relative to that of distilled water. The latter density is known from published tables.

Ultrasonic Pulse Spectroscopy for the Measurement of Phase Velocity and Attenuation

As discussed earlier in this paper, all the elastic parameters of a material can be calculated from the measurement of longitudinal and shear phase velocities. The technique described in the previous section is the conventional method of measuring the wave speed. If the specimen is thick (where the reflections can be separated in time domain), the transit time method is the easiest and very efficient. However, if the specimen is thin that method breaks down and cannot be used. Even when applicable, the conventional method requires human judgment and interference to make good measurements. The measurement of attenuation is not at all accurate and by this method only group velocity can be measured.

We have developed techniques which have eliminated all the above mentioned limitations. A fully computerized technique has been developed which can measure phase velocity and attenuation for thick as well as thin specimens. The digitized signal in time domain is transformed to the frequency domain by the use of Fast Fourier Transforms (FFT). If two pulses can be separated, then acoustic parameters, phase velocity, and attenuation are computed from the phase shift and loss of amplitude between two pulses in the reflected or transmitted signal. If the pulses cannot be separated, the complete signal is transformed by FFT and, by deconvolving the signal with respect to a reference signal, the acoustic parameters are computed. For details of these techniques readers are referred to Refs 12 and 13.

The techniques can be used both in the transmission and reflection mode. They can be used in direct contact or water immersion with a minor change in the governing equations. The techniques measure phase velocity and attenuation over a range of frequencies from which the group velocity can be obtained. Due to the fact that attenuation can be measured accurately, a variety of potential applications of this technique are envisaged. The effect of temperature up to the melting point of a material can be studied. The uni-

formity of the specimen and its porosity can be estimated. In composite materials we are able to assess damage due to mechanical and thermal loading. Brief accounts of the theory behind the technique, the procedure, and the results follow.

If the pulses can be separated in the time domain the following equation is obtained [13] for the water immersion reflection case:

$$G^*/F^* = 1 + T_{12}T_{21} \exp(-i2kh) \quad (10)$$

and for the direct contact reflection case:

$$G^*/F^* = 1 + R_{21}^2 \exp(-i2kh) \quad (11)$$

where

- G^* = FFT of two pulses,
- F^* = FFT of the first pulse,
- T_{ij} = transmission coefficient from medium i to j ,
- R_{ij} = reflection coefficient when the wave travelling in medium i reflects from i/j interface,
- h = specimen thickness,
- $k = k_1 + ik_2$ is the complex wavenumber,
- $k_1 = \omega/c$ is the wavenumber,
- ω = circular frequency,
- c = wave speed, and
- k_2 = attenuation.

Substituting $k = k_1 + ik_2$ into Eqs 10 and 11 and comparing the real and imaginary parts of the two sides, we obtain

$$k_1 = 2f/c = \phi/2h$$

$$\text{or } c = 4h/(\phi/f)$$

$$\text{and } k_2 = \ln(M)$$

where ϕ = phase of $G^*/F^* - 1$, and

$$M = \begin{cases} |G^*/F^* - 1|/(T_{12}T_{21}) & \text{in water immersion} \\ |G^*/F^* - 1|/R_{21}^2 & \text{in direct contact} \end{cases}$$

Similarly, if the pulse cannot be separated, then for the reflection field:

$$\exp(-i2kh) = [\beta/(1 + \beta)]R_{21}^2$$

where $\beta = R_{12}R_{21}[G^*/F^* - 1]/(T_{12}T_{21})$. Here G^* is the FFT of the entire reflected field and F^* is the FFT of the reference signal.

For the transmitted field:

$$\frac{\exp(-ih(k - k_0))}{1 - R_{21}^2 \exp(-i2kh)} = \frac{G^*}{T_{12}T_{21}F^*}$$

Here F^* is the FFT of the signal at the receiver when there is no sample between the two transducers and G^* is the FFT of the total transmitted signal after the specimen is introduced in the acoustic path.

Since fairly thick specimens were tested in the tests reported here, Eq 11 has been used in the measurements.

The block diagram of the experimental setup is as shown in Fig. 4. The analog signal is collected by the pulser-receiver and is fed

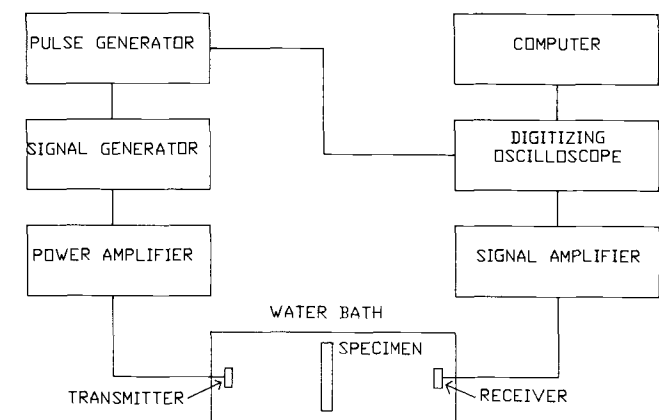


FIG. 4—Schematic diagram of the ultrasonic pulse spectroscopy technique.

into the digital oscilloscope. The signal is digitized in the oscilloscope. The signal processing unit of this oscilloscope performs Fast Fourier Transform on the signal. The useful portion of the transformed signal is then acquired by the computer for the calculation of the wave speed and the attenuation. In these steps several potential sources of errors can affect the results: (1) sampling interval, (2) frequency resolution, and (3) transducer response. The first factor is the digitizing interval of the acquired signal. The FFT of a 1 MHz signal at 10, 20, 40, and 100 ns sampling intervals was studied. It was observed that at the 10, 20, or 40 ns sampling interval the frequency content of the signal is essentially the same. However, at the 100 ns sampling interval, the signal loses some of its high frequency contents. The useful digitizing intervals depend on the frequency of the transducer being used. For example, for 10 MHz frequency, at the 40 ns interval some of the high frequency contents are lost. The second factor considered was the resolution of the signal in the frequency domain. A sampling interval of 40 ns or less with a frequency resolution of 0.05 MHz or less is considered adequate. This factor is also transducer frequency related. The third factor considered was the useful range of the transducer frequency response. It was found that satisfactory measurements can be obtained over a frequency range given by 25% of the peak response amplitude.

Three specimens were tested by the technique described above. The phase versus frequency plot for these specimens was a straight line; hence it can be deduced that the phase velocity ($\equiv \omega/k$) is equal to the group velocity ($\equiv d\omega/dk$) for these specimens.

The measurement of the wave speed is estimated to be accurate to $\pm 0.05\%$. The results obtained for three specimens are presented in Tables 3 and 4. The density for Specimens B2.2 and A1.3 was measured by the Archimedes principle; the density of Specimen A1.1 was measured by direct measurement of dimensions and mass. This resulted in a larger uncertainty in the measurement of density of Specimen A1.1 and consequently in a larger error in the value of E .

Piezoelectric Ultrasonic Composite Oscillator Technique (PUCOT)

Essentially, the apparatus for the PUCOT consists of piezoelectric quartz drive (D) and gage (G) crystals to excite longitudinal or torsional ultrasonic (kHz) resonant stress waves in the test speci-

men (S) of appropriate resonant length via a fused quartz spacer rod (Fig. 5). The components are joined with Loctite or ceramic cement as test temperature dictates. The spacer rod may be omitted for measurements near ambient temperatures. The resonant system is driven by a closed-loop oscillator which maintains a constant (preselected) gage voltage and hence a constant maximum strain amplitude in the specimen. During a test, values of the resonant period of the DGS (drive-gage-specimen) system are recorded and standard equations (Table 5) are used to calculate Young's modulus E . The validity of the measured value for E is determined from the ratio R of the period in the specimen to that of the quartz crystals. Ideally the ratio should be unity. However, ratios between 0.97 and 1.03 yield equally valid results. More detailed descriptions of the PUCOT have been given elsewhere [14-16].

The PUCOT is limited to frequencies between 20 and 200 kHz. Therefore specimens that resonate beyond this frequency range cannot be tested. The test specimen may be cylindrical or a parallelepiped, but the cross section can vary in size and shape. The ratio of specimen length to the largest dimension in the cross section must exceed five to prevent dispersion of the ultrasonic wave. The strain amplitude is in the range 10^{-8} to 10^{-4} .

The density of the specimens for the PUCOT study was determined by the Archimedes method.

Magnetically Excited Resonance

Magnetically excited resonance involves the use of an instrument known as the Modul-R which measures the longitudinal resonant frequency of a specimen of ferromagnetic material near 25 kHz. This frequency has been selected because it permits use of a convenient specimen length of about 100 mm. For convenience of calculations the specimen size is 104.63 by 6.35 mm. Thicknesses may vary from 0.203 to 2.03 mm. The specimen must be ferromagnetic because both the specimen drive and pickup signals are derived from magnetostriction in the specimen.

A schematic diagram of the apparatus is given in Fig. 6. The method of operation is as follows. The specimen is placed in the coil assembly where it is supported by the bias coil frame at its midlength location. A magnetic pulse initiates the vibration, setting up a field in the pickup coil from which a small signal is amplified and fed into the drive coil. An alternating current passing through the drive coil produces an alternating field in the interior of the coil. In the presence of this field, the specimen alternately contracts and extends longitudinally. These vibrations traverse the specimen with the velocity of sound and appear as vibrations in the part of the specimen encircled by the pickup coil. These changes in strain alter the permeability of the specimen and its magnetic flux density. The altered magnetic flux density induces an alternating current in the pickup coil by amplifying the pickup signal and feeding it back to the drive coil in the correct phase relationship with the mechanical vibrations initiated by the bias coil. The specimen becomes the frequency-controlling element of the magnetostrictive oscillator, and only the fundamental longitudinal resonant frequency is displayed on the digital output counter. On the basis of the results obtained for modulus with this technique, the magnetic field imposed on the specimen is small enough to avoid the ΔE effect.

For this interlaboratory study only Specimen B2.3 (ferromagnetic and of required dimensions) was tested with the Modul-R. The density of the specimen was determined by the Archimedes method.

TABLE 3—ASTM E28.03.05 dynamic Young's modulus interlaboratory study.

Alloy A		Raw Data Table		
Laboratory	Specimen	E, GPa	Density, g/cm ³	
1	1.1	218.0	8.43	IAI
	1.1	218.0	8.43	
	1.1	218.1	8.43	
	1.2	216.9	8.43	
	1.3	218.5	8.43	
2	1.1	210.5	8.376	Chen/Phillips
	1.3	209.2	8.339	
3	1.1	31.4*	8.43	Lemmens
	1.1	218.8	8.43	
	1.2	216.0	8.43	
	1.3	217.5	8.43	
	1.3	217.0	8.43	
	1.3	216.2	8.43	
	1.3	217.3	8.43	
4	1.1	212.0	8.36	NBS/Parallel
	1.3	205.0	8.36	NBS/Parallel
	1.3	215.0	8.36	NBS/Perpendicular, pos. 1**
	1.3	207.0	8.36	NBS/Perpendicular, pos. 2**
5	1.2	216.9	8.371	Texas A&M (PUCOT)
	1.4	216.6	8.373	
6	1.1	215.6	8.38	Texas A&M (Kinra)
	1.3	214.2	8.37	
7	1.1	203.0	8.25	3M
	1.3	210.3	8.37	

*Reject this value (wrong harmonic).

**See Fig. 3 for these positions.

Density listed for Laboratory 3 was determined at Laboratory 1.

Material: Inconel alloy 600, 25.4 mm diameter, hot-rolled annealed rod.

Specimens:

1.1: 6.35 mm diameter cylinder.

1.2: 25.4 mm diameter cylinder.

1.3: 3.18 by 6.35 by 101.6 mm flat strip.

1.4: 25.4 mm diameter cylinder (separate specimen for Laboratory 6).

Results

The results from the Interlaboratory Testing Program are quite voluminous. The data received from the various laboratories by the senior author were converted into values of Young's modulus by use of the various equations presented in the Experimental Procedures section. These values of modulus (and density) are listed in SI units in Tables 3 and 4. Finally, bar graphs of the Young's modulus measurements and the percentage deviations from the average values of the moduli for Materials A and B are presented in Figs. 7 to 10.

Analysis of Results and Discussion

Considering the wide variety of apparatus used in the eight laboratories, the results for dynamic Young's modulus of the two alloys are encouraging. Tables 3 and 4 show that the modulus ranges from 203 to 219 GPa for Material A and from 156 to 172 GPa for Material B. The mean and standard deviation for Material A are 213.91 and 4.46 GPa, respectively. It is interesting to note that the

deviations about the mean for Material A (Fig. 8) are all positive or all negative for a particular laboratory. While this result may suggest particular systematic errors associated with the apparatus at any given laboratory, this suggestion tends to be negated by an inspection of the deviations about the mean for Material B (Fig. 10). Here the deviations for four of the eight laboratories are both positive and negative.

A closer examination of Table 4 reveals that one of the results (2.3) for Laboratory 4 is outlying. Indeed, this was precisely the datum for which a poor signal was noted during testing (see section also for the comments on anisotropy and texture). Therefore it seems appropriate to discard this outlying result. When this is done, the deviations about the mean for Material B group closely (Fig. 10). The mean and standard deviation for the dynamic Young's modulus are 159.16 and 2.84 GPa, respectively, for Material B.

In connection with the adjustment of the data a very important point arises. The determination of the density of the specimen is an intrinsic part of modulus determination for *all* the techniques used. Therefore it is necessary to consider the density results from

TABLE 4—ASTM E28.03.05 dynamic Young's modulus interlaboratory study.

Alloy B		Raw Data Table		
Laboratory	Specimen	E, GPa	Density, g/cm ³	
1	2.1	161.5	8.34	IAI
	2.2	159.9	8.34	
	2.3	157.2	8.34	
2	2.1	164.1	8.392	Chen/Phillips
	2.3	155.7	8.225	
3	2.1	162.0	8.34	Lemmens
	2.1	161.8	8.34	
	2.1	160.8	8.34	
	2.3	158.4	8.34	
4	2.1	156.0*	8.25	NBS
	2.3	172.0**	8.25	
5	2.1	156.0	8.27	Texas A&M (PUCOT)
	2.3	162.0	8.26	
6	2.2	163.0	8.27	Texas A&M (Kinra)
7	2.1	156.8	8.20	3M
	2.3	155.8	8.17	
	2.3	158.0	8.17	
8	2.3	159.2	8.26	Modul-R

Density listed for Laboratory 3 was determined at Laboratory 1.

Material: Incoloy alloy 907, 19.05 mm thick, hot-rolled flat.

Specimens: 2.1: 6.35 mm diameter cylinder.

2.2: 25.4 mm diameter cylinder.

2.3: 1.91 by 6.35 by 101.6 mm flat strip.

*Wave propagation parallel to the length of the specimen.

**Wave propagation perpendicular to the length of the specimen.

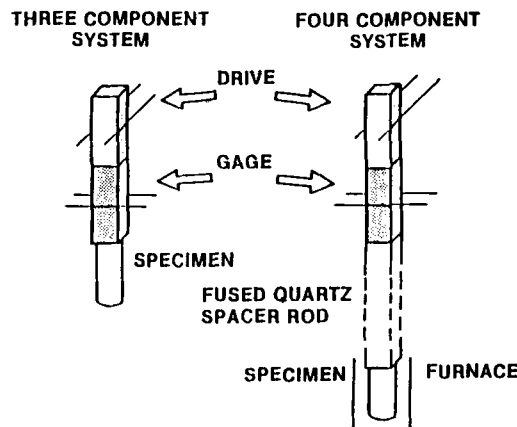


TABLE 5—PUCOT equations for the three-component system.

$$\begin{aligned}
 L &= (1/2f)(E/\rho)^{1/2} = \lambda/2 \\
 \tau(S) &= m(S)^{1/2} \tau(DG) \tau(DGS)/A \\
 A &= \{\tau(DG)^2 m(DGS) - \tau(DGS)^2 m(DG)\}^{1/2} \\
 E &= 4 \rho L^2 / \tau(S)^2 \\
 L &= \text{specimen length} \\
 f &= \text{frequency} \\
 E &= \text{Young's modulus} \\
 \rho &= \text{density} \\
 \lambda &= \text{wavelength} \\
 \tau &= \text{resonant period} \\
 S &= \text{specimen} \\
 D &= \text{drive crystal} \\
 G &= \text{gage crystal} \\
 m &= \text{mass}
 \end{aligned}$$

FIG. 5—Schematic diagram of the PUCOT. Left-hand side: three-component system for measurements at room temperature; right-hand side: four-component system for measurements at temperatures above room temperature. Shown is the arrangement with longitudinal quartz crystals.

all the laboratories in more detail. Figures 11 and 12 show bar charts of density for Materials A and B. For Material A the mean density was found to be 8.361 g/cm³ with a standard deviation of 0.048 g/cm³; the corresponding values for Material B are 8.263 and 0.072 g/cm³. Again it must be remembered that at some of the laboratories the Archimedes method of density determination was

used, while at others the density was determined from masses and physical dimensions of the specimens. That the deviations about the means for densities are mostly less than 0.08% is encouraging.

To proceed with the final adjustment of the dynamic Young's modulus data we have used what we term *common density* and *common mathematics*. *Common density* for the material is the value obtained by Laboratory 4 (NBS): Alloy A, 8.36 g/cm³; Alloy B, 8.25 g/cm³. (These values are very close to the means given in Figs. 11 and 12.) *Common mathematics* is a term indicating application of the same equations (including certain correction factors for shape and aspect ratio of the specimens, given by Spinner and

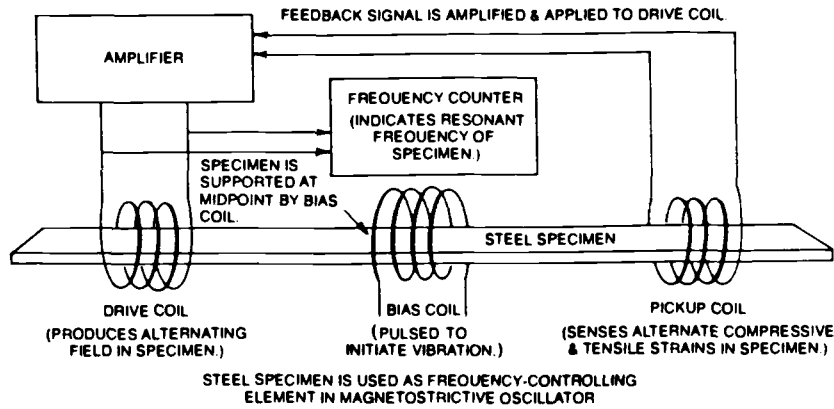


FIG. 6—Schematic diagram of the magnetically excited resonance system known as the Modul-R.

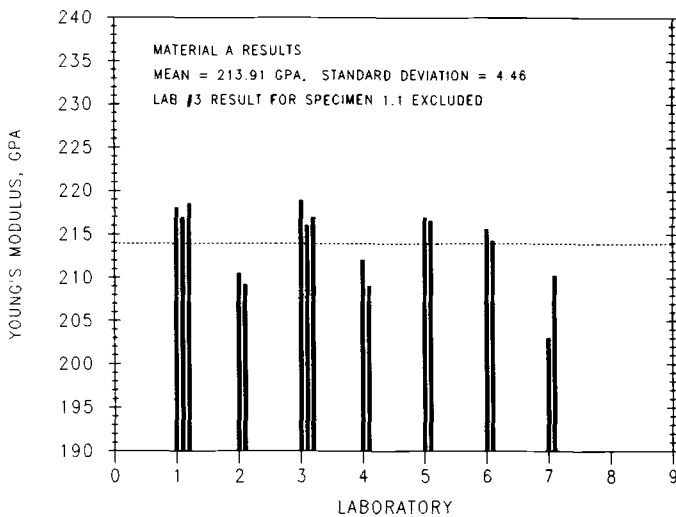


FIG. 7—Values of dynamic Young's modulus for Material A measured in the laboratories taking part in the testing program.

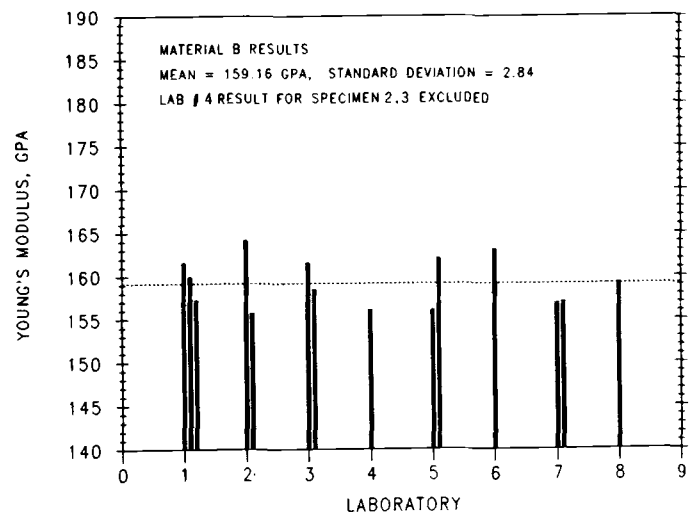


FIG. 9—Values of dynamic Young's modulus for Material B measured in the laboratories taking part in the testing program.

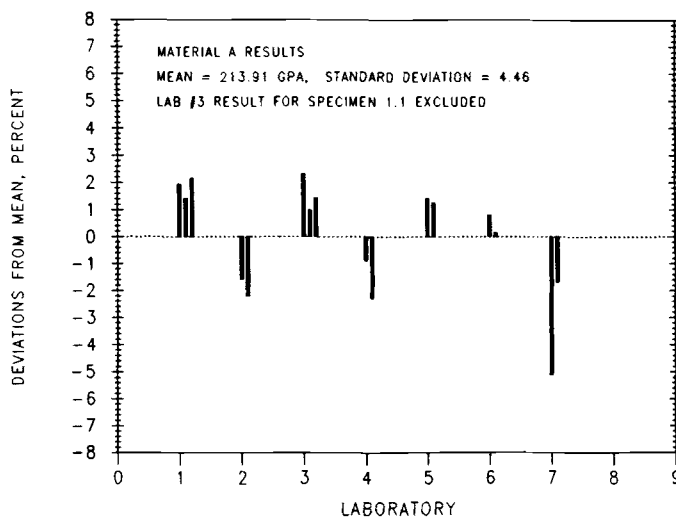


FIG. 8—Percentage deviations from the mean value of dynamic Young's modulus for Material A.

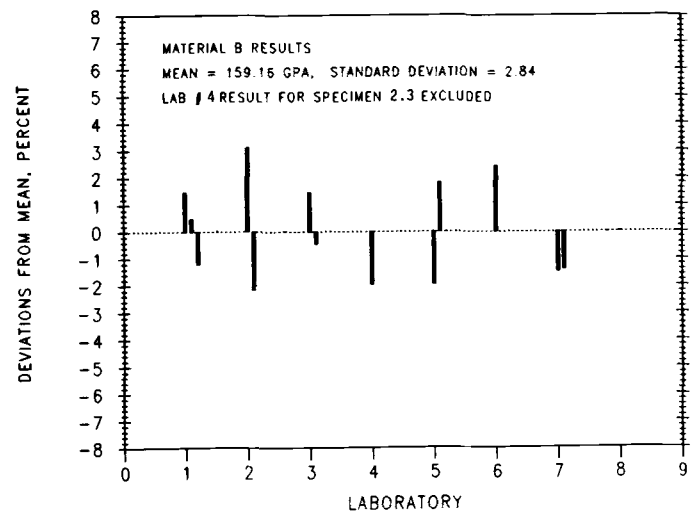


FIG. 10—Percentage deviations from the mean value of dynamic Young's modulus for Material B.

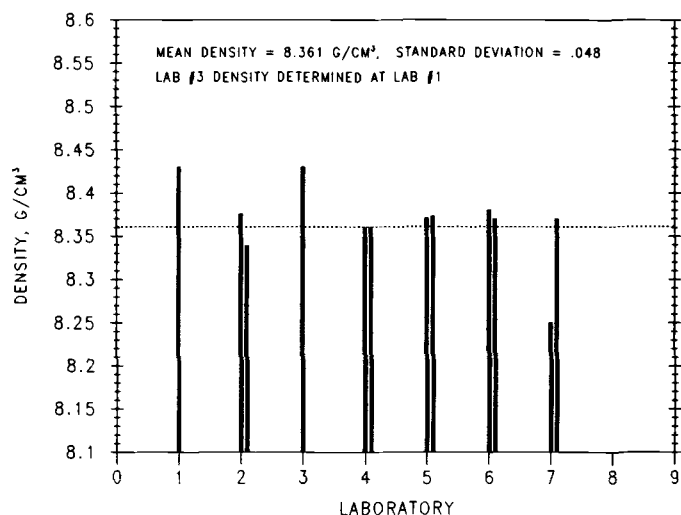


FIG. 11—Values of density determined for Material A at the various laboratories.

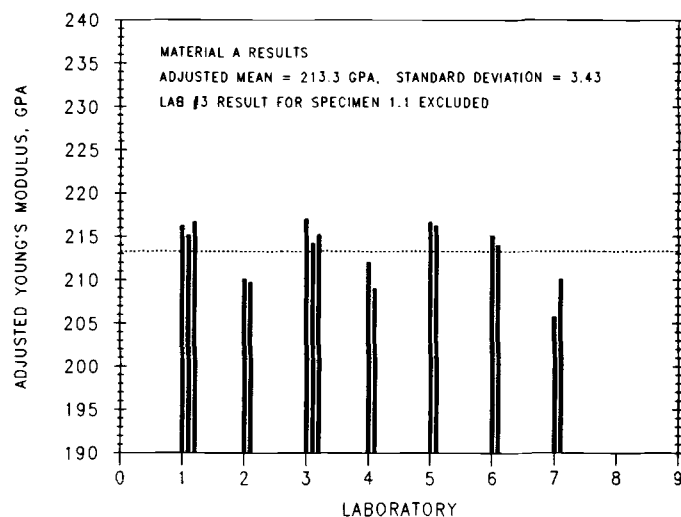


FIG. 13—Dynamic Young's modulus results for Material A with adjustments for common density and common mathematics.

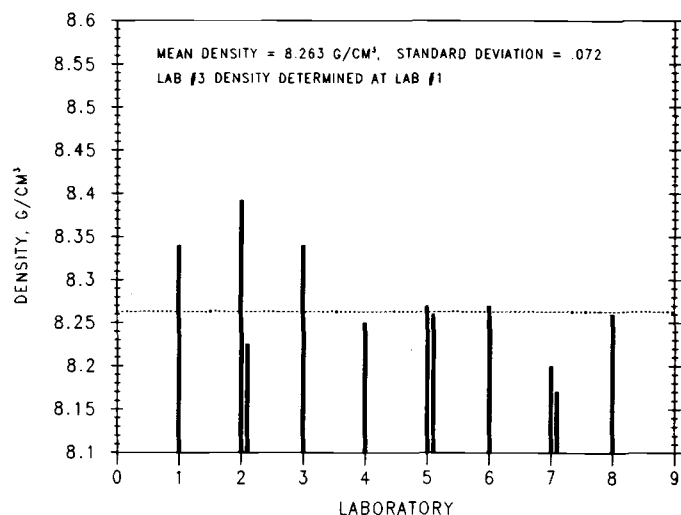


FIG. 12—Values of density determined for Material B at the various laboratories.

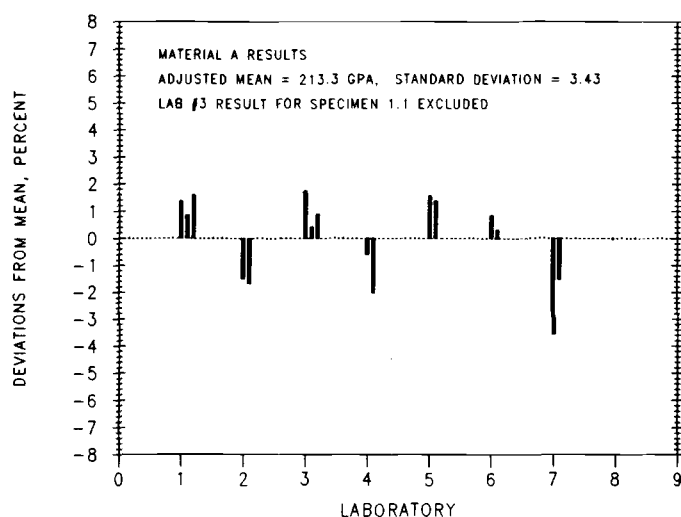


FIG. 14—Percentage deviations from the mean value of dynamic Young's modulus for Material A with adjustments for common density and common mathematics.

Tefft [2]) to convert measured values of frequency to values of modulus for the free-free beam technique (Laboratories 1, 2, and 7) and for the impulse technique (Laboratory 3). With these adjustments, the final results are presented in Figs. 13 to 16. For Alloy A the mean value of dynamic Young's modulus is 213.3 GPa with a standard deviation of 3.43 GPa (1.6%). The corresponding values for Alloy B are 160.59 and 2.37 GPa (1.5%), with the result for Specimen 2.3 from Laboratory 4 removed.

A further comment on the final adjustments of the dynamic Young's modulus data is in order. The value of modulus for Specimen A1.3 measured at Laboratory 7 was obtained using the first overtone rather than the fundamental. This would cause a lowering of the precision of the modulus value. The standard deviations (1.5 and 1.6%) about the means mentioned above are therefore larger than are potentially realizable by the dynamic techniques used.

To put a perspective on the quality of the results from this Inter-

laboratory Testing Program for dynamic Young's modulus, it is instructive to look at the results from the earlier round-robin study done at seven laboratories for static Young's modulus [17]. For the static modulus on a steel specimen the mean value was 211.3 GPa with a standard deviation of 5.1 GPa or 2.4%.

There does not appear to be any significant effect of frequency on the value of dynamic Young's modulus in the materials examined. Specifically, frequencies as low as 780 Hz (Laboratory 1) and as high as 15 MHz (Laboratory 4) were used for the modulus measurements, but no frequency dependence was established.

Conclusions

From this study of dynamic Young's modulus measurements, performed as an Interlaboratory Testing Program involving six types of apparatus, six different organizations, and specimens

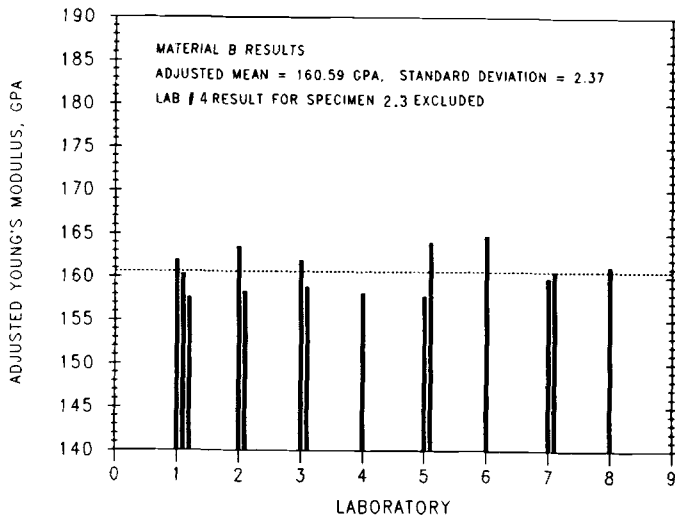


FIG. 15—Dynamic Young's modulus results for Material B with adjustments for common density and common mathematics.

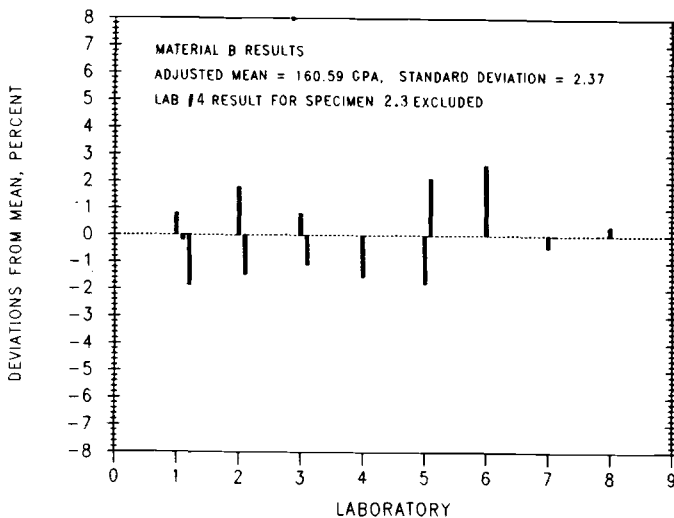


FIG. 16—Percentage deviations from the mean value of dynamic Young's modulus for Material B with adjustments for common density and common mathematics.

from a well-documented source, we can draw the following conclusions:

1. All the measurements of dynamic Young's modulus involved the basic wave equation (Eq 1) for the propagation of an elastic wave in an elastic medium.
2. The determination of the mass density of the specimens was an intrinsic part of the determination of dynamic Young's modulus for all the techniques used in this study.
3. All the techniques (free-free beam, impulse excitation, wave travel time, ultrasonic pulse spectroscopy, piezoelectric oscillation, and magnetically excited resonance) yielded values of dynamic Young's modulus that agreed closely with each other (to within 1.6%).
4. The mean value for dynamic Young's modulus for Inconel 600 (Alloy A) was determined as 213.3 GPa with a standard deviation of 3.4 GPa, while the corresponding values for Incoloy 907 (Alloy B) were 160.6 and 2.4 GPa, respectively. These modulus values are based on the density values of 8.36 and 8.25 g/cm³ for Materials A and B, respectively, measured at NBS, and on common mathematical equations for certain techniques used in this study.

5. There does not appear to be any significant effect of frequency on dynamic Young's modulus in the materials tested for the frequency range 780 Hz to 15 MHz.

Acknowledgments

We are grateful to the following colleagues, most of them members of ASTM, who have contributed valuable time and advice during the period of the Interlaboratory Study: A. Fox, R. Willoughby, M. E. Lieff, J. A. Millane, T. Mellon, R. Kennedy, E. Dietrich, E. W. Filer, G. Hickcock, D. Dineff, R. Gassner, R. G. Baughan, D. DeMiglio, W. T. Groor, D. Scanlon, R. S. Strimel, S. B. Helms, W. Engelmaier, D. Germano, W. Pearce, J. E. Amaral, J. Moch, A. Perlov, N. L. Carroll, G. Foster, R. Papirno, W. Stange, T. Finke, D. Bray, J. D. Whittenberger, G. M. Ludtka, and L. Mordfin. Special thanks go to Inco Alloys International (IAI) for provision of specimens, to Dr. P. Ganesan for texture information, and to R. S. Davis of NBS for the values of common density used in the final analysis. M. D. Wyrick was responsible for the modulus measurements at IAI. Two of us (V.K.K. and V.D.) acknowledge financial support by the Air Force Office of Scientific Research under Contract F49620-83-C-0067 to Texas A&M University, College Station, Texas. The authors are most grateful to the reviewers of the manuscript for many helpful suggestions for its improvement.

References

- [1] Pickett, G. in *Proceedings of ASTM*, Vol. 45, 1945, pp. 846-865.
- [2] Spinner, S. and Tefft, W. E. in *Proceedings of ASTM*, Vol. 61, 1961, pp. 1221-1238.
- [3] Wagel, R. L. and Walther, H., *Physics*, Vol. 6, 1935, pp. 141-157.
- [4] Harris and Crede, *Shock and Vibration Handbook*, Vol. 1, pp. 1-14.
- [5] Dickson, R. W. and Spinner, S., *Journal of Materials*, Vol. 3, Sept. 1968, pp. 716-724.
- [6] Kolsky, H., *Stress Waves in Solids*, Dover Publications, New York, 1963.
- [7] Szilard, J. in *Ultrasonic Testing: Non-Conventional Testing Techniques*, J. Szilard, Ed., Chapters 1, 2, and 9, Wiley, New York, 1982.
- [8] Papadakis, E. P. in *Physical Acoustics Principles and Methods*, W. P. Mason and R. N. Thurston, Eds., Vol. 12, Chapter 5, Academic Press, New York, 1976.
- [9] Papadakis, E. P., *Transactions of IEEE*, Vol. SU-16, 1969, pp. 210-218.
- [10] Papadakis, E. P. in *Physical Acoustics Principles and Methods*, W. P. Mason and R. N. Thurston, Eds., Vol. 11, Chapter 3, Academic Press, New York, 1975.
- [11] Papadakis, E. P., *Journal of the Acoustical Society of America*, Vol. 42, 1967, pp. 1045-1051.
- [12] Dayal, V., Kinra, V. K., and Eden, J. G., "Ultrasonic Nondestructive Testing of Fiber Reinforced Composites," in *Proceedings, International Symposium on Composite Materials*, Beijing, 1986, pp. 899-904.
- [13] Kinra, V. K. and Dayal, V., "A New Technique for Ultrasonic NDE of Thin Specimens," *Experimental Mechanics*, Sept. 1988, pp. 288-297.
- [14] Marx, J., *Review of Scientific Instruments*, Vol. 22, 1951, pp. 503-509.
- [15] Robinson, W. H. and Edgar, A., *IEEE Transactions of Sonics and Ultrasonics*, Vol. SU-21, 1974, pp. 98-105.
- [16] Harmouche, M. R. and Wolfenden, A., *Journal of Testing and Evaluation*, Vol. 13, 1985, pp. 424-428.
- [17] ASTM Static Modulus Study (E28.03).